Available online at www.derpharmachemica.com

Scholars Research Library

Der Pharma Chemica, 2014, 6(3):373-384
(http://derpharmachemica.com/archive.html)

ISSN 0975-413X
CODEN (USA): PCHHAX

Anticorrosive properties of 3-hydroxy-7-isocyano-8-phenyl-2-(p-tolyl)pyrimido[2,1-b][1,3]thiazine-4,6-dione on carbon steel in 1.0 M HCl Solution

M. Larouj [1*], M. Belayachi [1], H. Zarrok [1], A. Zarrouk [2,], A. Guenbour [3], M. Ebn Touhami [4], A. Shaim [5], S. Boukhriss [6], H. Oudda [1], B. Hammouti [2]

[1] Laboratoire de Procédés de Séparation, Faculté des Sciences, Université Ibn Tofail, 133, 14000 Kénitra, Maroc
[3] LCAE-URAC18, Faculté des Sciences, Université Mohammed 1er, Oujda, Morocco.
[3]Laboratoire d'Electrochimie, Corrosion et Environnement, Faculté des Sciences, Rabat, Morocco.
[4]Laboratoire d'électrochimie, de corrosion et d'environnement, Faculté des Sciences, Université Ibn Tofail BP 242, 14000 Kenitra, Morocco.
[5]Laboratoire de Physico-Chimie du Solide (LPCS), Faculté des Sciences, Université Ibn Tofail, B.P. 133, 14000 Kenitra, Morocco.
[6] Equipe de Synthèse Organique, Organométallique et théorique, Faculté des Sciences, Université Ibn Tofail, BP 133, 14000 Kénitra, Maroc.

ABSTRACT

Electrochemical impedance spectroscopy (EIS) and potentiodynamic polarization (PDP) studies were carried out to investigate the comparative corrosion protection efficiency of 3-hydroxy-7-isocyano-8-phenyl-2-(p-tolyl)pyrimido[2,1-b][1,3]thiazine-4,6-dione (HPPTD) on carbon steel in 1.0 M HCl. EIS plots indicated that the addition of this inhibitor increases the charge-transfer resistance (R_{ct}), decreases the double-layer capacitance (C_{dl}) of the corrosion process, and hence increases inhibition performance. At 303 K, polarization measurements indicated that this compound is mixed-type inhibitor. Moreover, the thermodynamic activation parameters for the corrosion reaction were calculated and discussed in relation to the stability of the protective inhibitor layer. The adsorption of the studied pyrimidothiazine derivative obeyed the Langmuir adsorption isotherm.

***Keywords**: Pyrimidothiazine inhibitor, Carbon steel, HCl, EIS, Polarization.*

INTRODUCTION

Acid solutions are widely used for industrial cleaning, for oil well acidification, and in petroleum processes [1,2]. Hydrochloric acid is generally used in the pickling processes of metals and alloys [3,4], because of their aggressiveness; inhibitors are used to reduce the rate of dissolution of metals. The use of organic molecules as corrosion inhibitors is one of the most practical methods for protecting metals against corrosion, and it is becoming increasingly popular [5-25]. The adsorption of these molecules depends mainly on certain physicochemical properties of the inhibitor molecules such as functional groups, steric factors, aromaticity, electron density at the donor atoms, π-orbital character of donating electrons, and electronic structures of the molecules [26-31].

Investigations of more environmentally acceptable corrosion inhibitors are of great practical interest. One of the effective methods to prevent corrosion is the use of organic inhibitors. It has been widely seen that organic

molecules containing heteroatoms such as nitrogen, sulfur, or oxygen as well as heterocyclic aromatic ring systems containing conjugated double bonds have been reported as good inhibitors for carbon steel [32,33].

The present investigation was undertaken to examine the corrosion inhibition capacity of a heterocyclic 3-hydroxy-7-isocyano-8-phenyl-2-(p-tolyl)pyrimido[2,1-b][1,3]thiazine-4,6-dione (HPPTD) in 1.0 M HCl solution on carbon steel at 303-333 K using potentiodynamic polarisation (PDP) curves and electrochemical impedance spectroscopy (EIS) methods. The adsorption isotherm of inhibitor on steel surface was determined. Kinetic parameters are calculated and discussed in detail. Figure 1 shows the molecular structure of the pyrimidothiazine derivative utilised in this investigation.

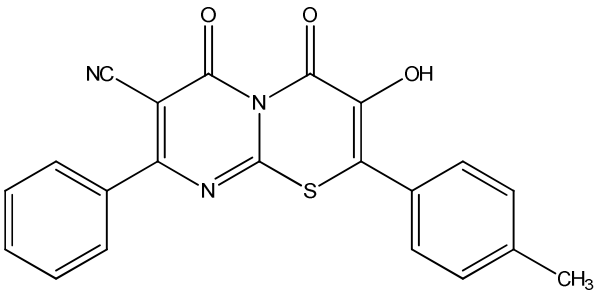

Figure 1. Structure of 3-hydroxy-7-isocyano-8-phenyl-2-(p-tolyl)pyrimido[2,1-b][1,3]thiazine-4,6-dione

MATERIALS AND METHODS

Materials

The steel used in this study is a carbon steel (CS) (Euronorm: C35E carbon steel and US specification: SAE 1035) with a chemical composition (in wt%) of 0.370 % C, 0.230 % Si, 0.680 % Mn, 0.016 % S, 0.077 % Cr, 0.011 % Ti, 0.059 % Ni, 0.009 % Co, 0.160 % Cu and the remainder iron (Fe).

Synthesis

Pyrimidin-4-ones, by virtue of their ambident nucleophilic centers, are good starting materials for the synthesis of several interesting N and S-bridged heterocycles. Also, we have designed a simple method for the synthesis of 3-hydroxy-4,6-dioxo-8-phenyl-2-(p-toly)-4,6-dihydropyrimido [2,1-b][1,3]thyazine-7-carbonitrile (HDPDTC) by the reaction of gem-cyanoester epoxide 1 with the pyrimidin-4-one 2.

Indeed, treatment of 2 with one equivalent of pyrimidin-4-one 2 in acetonitrile under reflux for 3h afforded product identified as 3-hydroxy-4,6-dioxo-8-phenyl-2-(p-toly)-4,6-dihydropyrimido [2,1-b][1,3]thyazine-7-carbonitrile (HDPDTC). Scheme 1 shows that the reaction proceeds by the regioselective opening of the epoxide initiated by the sulfur atom followed by that of nitrogen atom of pyrimidin-4-one 2 leading to 3-hydroxy-4,6-dioxo-8-phényl-2-(p-toly)-4,6-dihydropyrimido[2,1-b][1,3]thyazine-7-carbonitrile through cyanhydrins and α-ketoesters as intermediates [34].

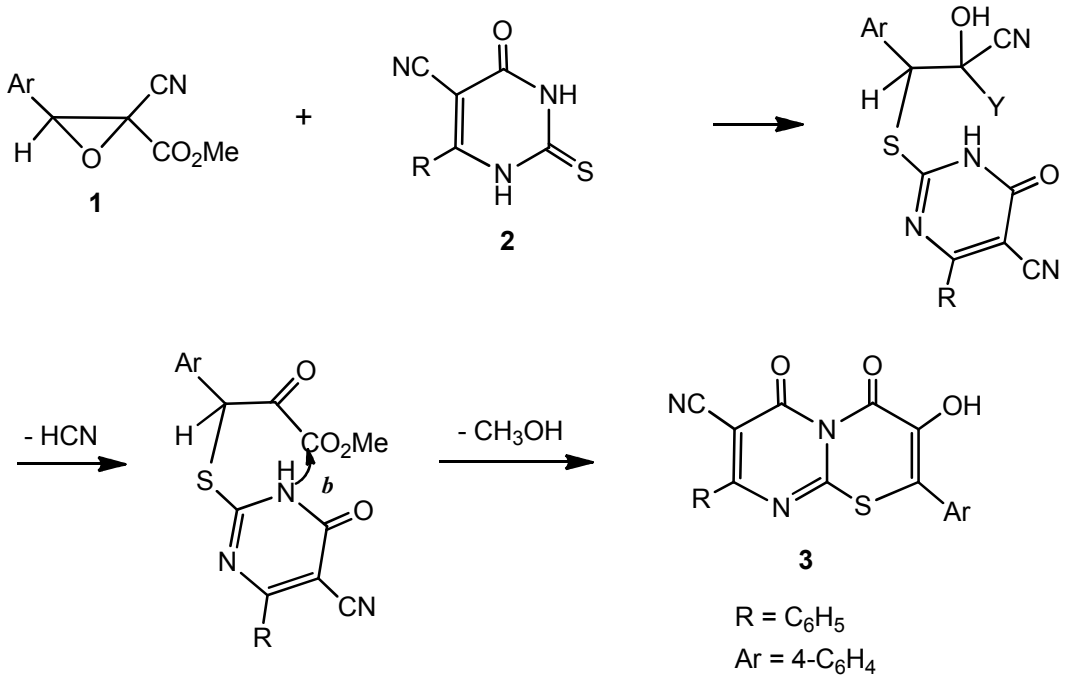

Scheme 1. Synthesis of new pyrimidothiazine derivative.

Solutions

The aggressive solutions of 1.0 M HCl were prepared by dilution of analytical grade 37% HCl with distilled water. The concentration range of 3-hydroxy-7-isocyano-8-phenyl-2-(p-tolyl)pyrimido[2,1-b][1,3]thiazine-4,6-dione (HPPTD) used was 10^{-6} M to 10^{-3} M.

Polarization measurements

Electrochemical impedance spectroscopy

The electrochemical measurements were carried out using Volta lab (Tacussel- Radiometer PGZ 100) potentiostate and controlled by Tacussel corrosion analysis software model (Voltamaster 4) at under static condition. The corrosion cell used had three electrodes. The reference electrode was a saturated calomel electrode (SCE). A platinum electrode was used as auxiliary electrode of surface area of 1 cm^2. The working electrode was carbon steel. All potentials given in this study were referred to this reference electrode. The working electrode was immersed in test solution for 30 minutes to a establish steady state open circuit potential (*E*ocp). After measuring the *E*ocp, the electrochemical measurements were performed. All electrochemical tests have been performed in aerated solutions at 303 K. The EIS experiments were conducted in the frequency range with high limit of 100 kHz and different low limit

0.1 Hz at open circuit potential, with 10 points per decade, at the rest potential, after 30 min of acid immersion, by applying 10 mV ac voltage peak-to-peak. Nyquist plots were made from these experiments. The best semicircle can be fit through the data points in the Nyquist plot using a non-linear least square fit so as to give the intersections with the *x*-axis.

The inhibition efficiency of the inhibitor was calculated from the charge transfer resistance values using the following equation [35]:

$$\eta_z\% = \frac{R_{ct}^i - R_{ct}^\circ}{R_{ct}^i} \times 100 \qquad (1)$$

where, R_{ct}° and R_{ct}^i are the charge transfer resistance in absence and in presence of inhibitor, respectively.

Potentiodynamic polarization

The electrochemical behaviour of carbon steel sample in inhibited and uninhibited solution was studied by recording anodic and cathodic potentiodynamic polarization curves. Measurements were performed in the 1.0 M HCl solution containing different concentrations of the tested inhibitor by changing the electrode potential automatically from -

900 to -100 mV versus corrosion potential at a scan rate of 1 mV s^{-1}. The linear Tafel segments of anodic and cathodic curves were extrapolated to corrosion potential to obtain corrosion current densities (I_{corr}). From the polarization curves obtained, the corrosion current (I_{corr}) was calculated by curve fitting using the equation:

$$I = I_{corr}\left[exp\left(\frac{2.3\Delta E}{\beta_a}\right) - exp\left(\frac{2.3\Delta E}{\beta_c}\right)\right] \quad (2)$$

The inhibition efficiency was evaluated from the measured I_{corr} values using the relationship:

$$\eta_{Tafel}\% = \frac{I^{\circ}_{corr} - I^{i}_{corr}}{I^{\circ}_{corr}} \times 100 \quad (3)$$

where, I°_{corr} and I^{i}_{corr} are the corrosion current density in absence and presence of inhibitor, respectively.

RESULTS AND DISCUSSION

Electrchemical Impedance Spectroscopy (EIS)

Electrochemical impedance spectroscopy (EIS) is an effective method for corrosion studies of metallic materials. The effect of HPPTD concentration on the impedance spectra of carbon steel in 1.0 M HCl solutions at 303 K is recorded in Fig. 2 (Nyquist plots). It is clear to see that the impedance spectra are significantly changed with addition of different HPPTD concentration. From the Nyquist plots, it was also observed that, even the presence of HPPTD does not alter the style of impedance plots, thus indicating the addition of HPPTD does not change the mechanism for the dissolution of carbon steel in 1.0 M HCl solution [36,37].

The impedance diagrams show only one capacitive loop represented by slightly depressed semicircle which indicates that the corrosion of carbon steel in 1.0 M HCl solution is mainly controlled by charge transfer process and formation of a protective layer on the carbon steel surface. The diameter of the capacitive loop increases with the increase of HPPTD concentration proposing that the formed inhibitive film was strengthened by the addition of HPPTD [38]. The depressed semicircles are generally attributed to the frequency dispersion as well as roughness and inhomogeneities of solid surface, and mass transport process [39], distribution of the active sites, adsorption of inhibitors [40-42]. The adsorption of this inhibitor on the carbon steel surface decreases its electrical capacity because of the displacement of water molecule and other ions originally adsorbed on the metal surface. The decrease in this capacity with increase in inhibitory concentration may be attributed to the formation of a protective film on the electrode surface [43]. The thickness of this protective layer increases with increase in inhibitor concentration, as more pyrimidothiazine derivative electro statically adsorbed on the electrode surface, resulting in a noticeable decrease in C_{dl}. This trend is in accordance with Helmholtz model given by the equation:

$$\delta_{org} = \frac{\varepsilon_0 \varepsilon_r}{C_{dl}} \times A \quad (4)$$

where $\boldsymbol{\varepsilon_0}$ is the vacuum dielectric constant, ε_r is the local dielectric constant, δ_{org} is the thickness of the double layer, and **A** is the surface area of the electrode.

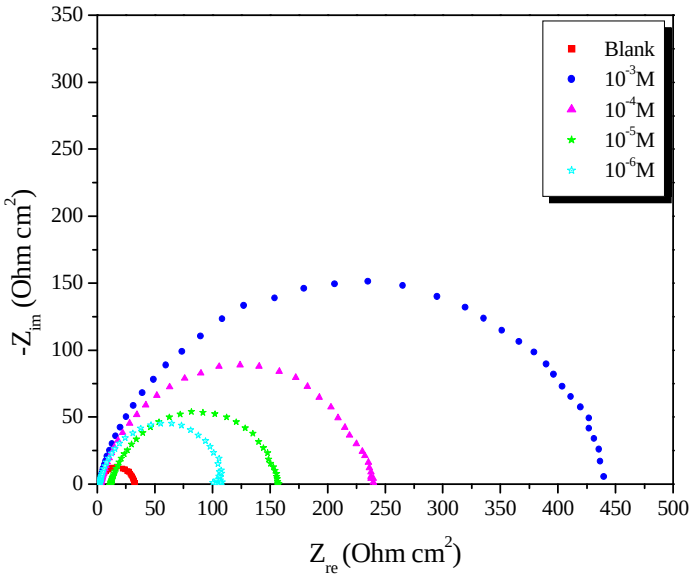

Figure 2. Nyquist digrams Steel in 1.0 M HCl without and with different concentrations of HPPTD.

Table 1. Electrochemical impedance parameters and inhibition efficiency for carbon steel in 1.0 M HCl solution with HPPTD at 303K.

	Conc (M)	R_{ct} (Ω cm^2)	f_{max} (Hz)	C_{dl} (μF/cm^2)	η_z (%)
Blank	1.0	32.8	63.34	80.99	-----
HPPTD	10^{-3}	459.0	1.25	18	93
	10^{-4}	242.0	3.16	34	86
	10^{-5}	157.7	1.25	61	79
	10^{-6}	108.0	2.50	69	70

Potentiodynamic polarization measurements

Effect of concentration inhibitor

Figure 3 illustrates the polarization curves of carbon steel in 1.0 M HCl solution without and with various concentrations of HPPTD at 303 K. The presence of HPPTD shifts both anodic and cathodic branches to the lower values of corrosion current densities and thus causes a remarkable decrease in the corrosion rate. The parameters derived from the polarization curves in Figure 3 are given in Table 2. In 1.0 M HCl solution, the presence of HPPTD causes a remarkable decrease in the corrosion rate i.e., shifts both anodic and cathodic curves to lower current densities. In other words, both cathodic and anodic reactions of carbon steel electrode are retarded by HPPTD in hydrochloric acid solution. The Tafel slopes of β_c at 303 K change remarkably upon addition of HPPTD, which indicates that, the presence of HPPTD change the mechanism of hydrogen evolution and the metal dissolution process. Generally, an inhibitor can be classified as cathodic or anodic type if the shift of corrosion potential in the presence of the inhibitor is more than 85 mV with respect to that in the absence of the inhibitor [44,45]. In the presence of HPPTD, E_{corr} shifts to less negative but this shift is lower (about 6-81 mV) which indicates that HPPTD can be arranged as a mixed type inhibitor, with predominant cathodic effectiveness.

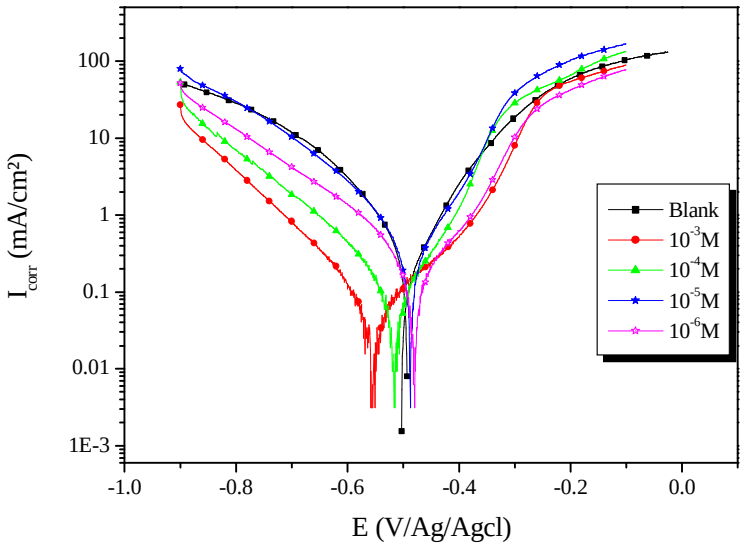

Figure 3. Polarisation curves for carbon steel in 1.0 M HCl in the absence and presence of different concentrations of HPPTD at 303K.

Table 2. Polarisation data of carbon steel in 1.0 M HCl without and with addition of inhibitor at 303 K.

Inhibitor	Conc (M)	$-E_{corr}$ (mV/Ag/AgCl)	$-\beta_c$ (mV/dec)	I_{corr} ($\mu A\ cm^{-2}$)	η_{Tafel} (%)	θ
Blank	1.0	475.9	175.6	1077.8	-----	-----
HPPTD	10^{-3}	556	118	57	94.7	0.947
	10^{-4}	517	99	100	90.7	0.907
	10^{-5}	481	86	114	89.4	0.894
	10^{-6}	521	95	180	83.3	0.833

Effect of temperature

The effect of temperature on the various corrosion parameters E_{corr}, I_{corr} and η_{Tafel} (%) was studied in 1.0 M HCl at temperature range 303-333 K in the absence and presence of 1.0 mM of HPPTD (Figs. 4 and 5). Variation of temperature has almost no effect on the general shape of the polarization curves. The results were listed in Table 3. An inspection of Table 3 shown that, as the temperature increased, the values of E_{corr} shift in the negative direction, while the values of I_{corr} increase and η_{Tafel} (%) decrease. This behaviour reflects physical adsorption of HPPTD on the steel surface.

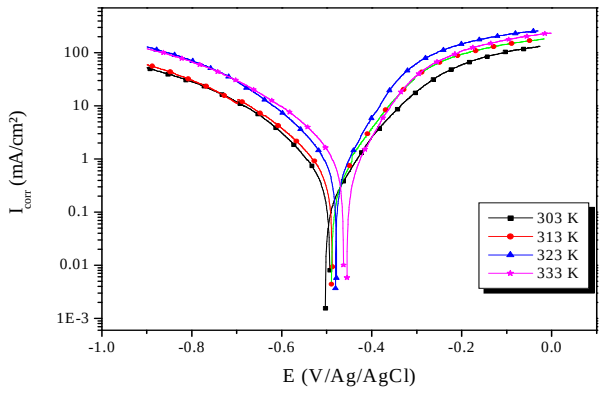

Figure 5. Potentiodynamic polarisation curves of carbon steel in 1.0 M HCl at different temperatures.

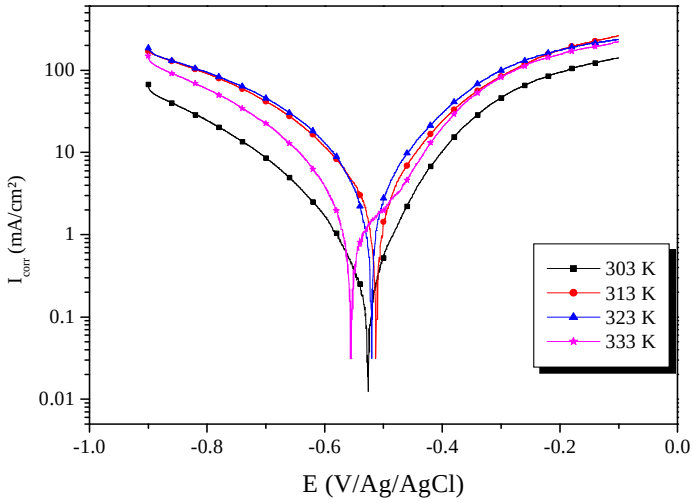

Figure 6. Potentiodynamic polarisation curves of carbon steel in 1.0 M HCl in the presence of 10^{-3} M of HPPTD at different temperatures.

Table 3. The influence of temperature on the electrochemical parameters for carbon steel electrode immersed in 1.0 M HCl and 1.0 M HCl + 1.0 mM of HPPTD.

	Temp (K)	$-E_{corr}$ (mV/Ag/AgCl)	I_{corr} (μA cm^{-2})	η_{Tafel} (%)
Blank	303	498	1077.8	----
	313	490	1200	----
	323	481	1300	----
	333	459	1400	----
HPPTD	303	556	57	94.7
	313	516	240	80.0
	323	533	300	77.0
	333	530	500	64.3

The mechanism of the inhibitor action can be deduced by comparing the apparent activation energies, E_a, in the presence and absence of the corrosion inhibitor. Activation parameters such as E_a, the enthalpy of activation, ΔH_a, and the entropy of activation, ΔS_a, for both corrosion and corrosion inhibition of carbon steel in 1.0 M HCl in the absence and presence of 1.0 mM concentration of HPPTD in the range of temperatures (303 to 333K) were calculated from an Arrhenius-type plot (eq. 5) and transition state (eq. 6), respectively. Figures 4 and 5 represent the data plots of Ln (I_{corr}) versus 1000/T and Ln (I_{corr}/T) versus 1000/T, respectively, in the absence and presence of 1.0 mM concentration of this inhibitor. The calculated values of E_a, ΔH_a and ΔS_a are tabulated in Table 4.

$$I_{corr} = k \exp\left(-\frac{E_a}{RT}\right) \quad (5)$$

$$I_{corr} = \frac{RT}{Nh}\exp\left(\frac{\Delta S_a}{R}\right)\exp\left(\frac{\Delta H_a}{RT}\right) \quad (6)$$

where E_a is the apparent activation corrosion energy, T is the absolute temperature, k is the Arrhenius pre-exponential constant, R is the universal gas constant, h is Planck's constant, N is Avagadro's number, ΔS_a is the variation of entropy of activation and ΔH_a is the variation of enthalpy of activation.

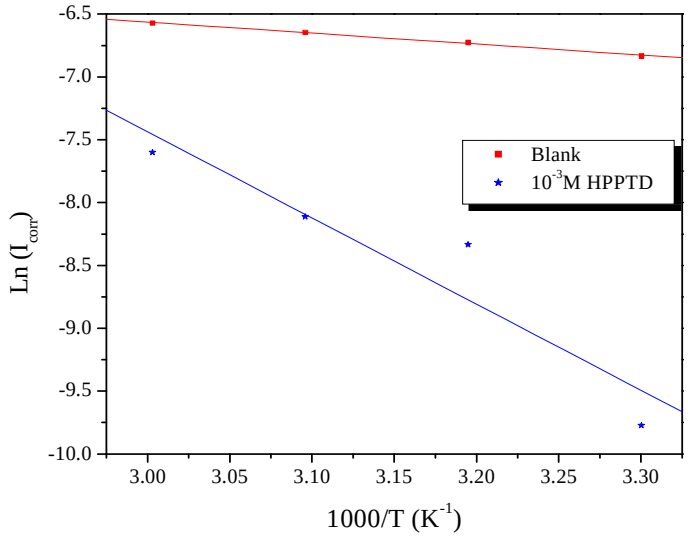

Figure 7. Arrhenius plots for carbon steel in 1.0 M HCl in the absence and presence of 1.0 mM concentration of HPPTD.

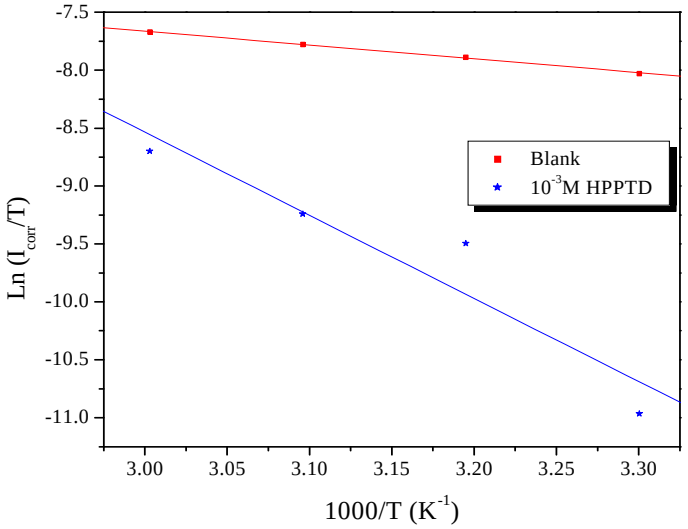

Figure 8. Transition state plots for carbon steel in 1.0 M HCl in the absence and presence of 1.0 mM concentration of HPPTD.

Table 4. Activation parameters, E_a, ΔH_a and ΔS_a, of the dissolution of carbon steel in 1.0 M HCl in the absence and the presence of 1.0 mM of HPPTD.

Inhibitor	E_a (kJ/mol)	ΔH_a (kJ/mol)	ΔS_a (J mol^{-1} K^{-1})
Blank	7.3	10.0	-231.5
HPPTD	57	59.6	-89.7

Inspection of Table 4 shows that values of both E_a and ΔH_a obtained in presence of HPPTD are higher than those obtained in the inhibitor-free solutions. This observation further supports the proposed physical mechanism. Higher values of E_a suggests a physical adsorption mechanism [46], while unchanged or lower values of E_a in inhibited systems compared to the blank has been reported [47-49] to be indicative of chemisorption mechanism. On the other hand, the positive value of ΔH_a reflects the endothermic nature of the carbon steel dissolution process [50], while the increase of ΔS_a reveals that an increase in disordering takes place on going from reactant to the activated complex [51]. This behavior can be explained as a result of the replacement process of water molecules during adsorption of HPPTD on steel surface. One can notice that E_a and ΔH_a values vary in the same way (Table 4).

Effect of immersion time

Figure 9 shows the impedance spectra at different immersion time in 1.0 M HCl containing 10^{-3} M of HPPTD. It is marked that these diagrams exhibit one capacitive loop. It is also note that the increasing of immersion time affects the diameter loops.

The variation of inhibition efficiency with temperature is given in Table. It is clear from the table that the increase in the immersion time does not affect much on the inhibition efficiency. These results demonstrate that the formation of surface film, and therefore the HPPTD adsorption, on the electrode surface is stable with immersion time.

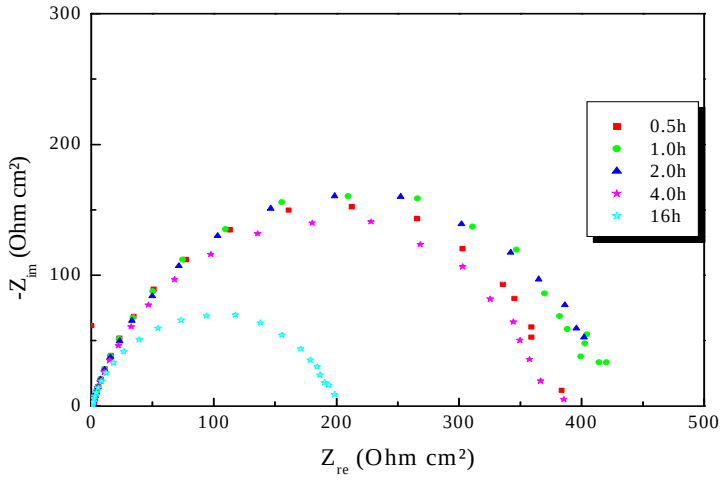

Figure 9. Effect of immersion time on the behaviour of the carbon steel / 1.0 M HCl interface in the presence of 10^{-3}M of inhibitor

Adsorotion isotherm

In order to gain more information about the mode of adsorption of HPPTD on the surface of carbon steel at different temperatures, the experimental data have been tested with several adsorption isotherms. In order to obtain the isotherm, coverage θ as a function of HPPTD concentration must be obtained. Coverage can be obtained from polarization measurement by the following equation [52]:

$$\theta = \frac{I^{\circ}_{corr} - I^{i}_{corr}}{I^{\circ}_{corr}} \qquad (7)$$

where, I°_{corr} and I^{i}_{corr} are the corrosion current density in absence and presence of inhibitor, respectively. The best fit was obtained with Langmuir adsorption isotherm as in Fig. 10. According to Langmuir isotherm, Coverage θ is related to inhibitor concentration C_{inh} by the following relation [52]:

$$\frac{\theta}{1-\theta} = K_{ads} C_{inh} \qquad (8)$$

and rearranging it gives

$$\frac{C_{inh}}{\theta} = \frac{1}{K_{ads}} + C_{inh} \qquad (9)$$

where K_{ads} is the equilibrium constant of the adsorption process.

Fig. 10 shows the plots of C_{inh}/θ against inhibitor concentration C_{inh} at 303K and the expected linear relationship is obtained for this compound with excellent correlation coefficent (R^2) (Table 5), confirming the validity of this approach. The slope of the straight lines is unity, suggesting that adsorbed inhibitor molecules form monolayer on the carbon steel surface and there is no interaction among the adsorbed inhibitor molecules.

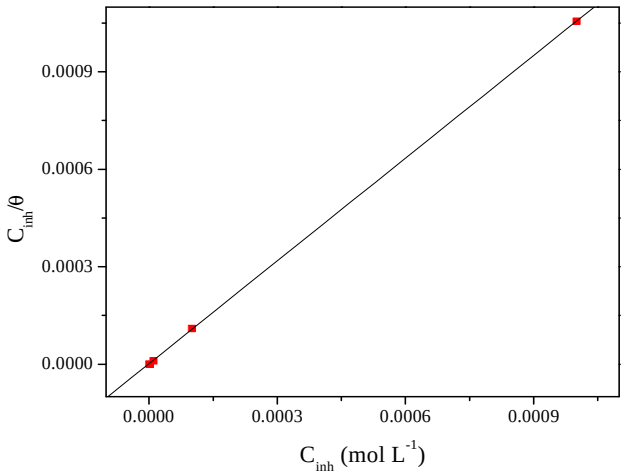

Figure 10. Langmuir adsorption of HPPTD on the carbon steel surface in 1.0 M HCl solution.

Table 5. Langmuir adsorption parameters.

Inhibitor	Slope	K_{ads} (M^{-1})	R^2	ΔG°_{ads} (kJ/mol)
HPPTD	1.05	565991.82	0.99999	-43.49

The value of K_{ads} obtained from the Langmuir is listed in Table 5, together with the value of the Gibbs free energy of adsorption (ΔG°_{ads}) calculated from the equation [53]:

$$\Delta G^{\circ}_{ads} = -RTLn(55.5K_{ads}) \qquad (10)$$

where R is gas constant and T is absolute temperature of experiment and the constant value of 55.5 is the concentration of water in solution in mol L^{-1} [54].

The high value of K_{ads} for studied pyrimidothiazine derivative indicate stronger adsorption on the carbon steel surface in 1.0 M HCl solution. This can be explained by the presence of heteroatoms and π-electrons in the inhibitor molecules. Large value of K_{ads} imply more efficient adsorption hence better inhibition efficiency [55]. The large value of K_{ads} obtained for the pyrimidothiazine derivative agrees with the high inhibition efficiency obtained.

The negative value of ΔG°_{ads} calculated from Eq. (10), are consistent with the spontaneity of the adsorption process and the stability of the adsorbed layer on the carbon steel surface. Generally, values of ΔG°_{ads} up to -20 kJ mol^{-1} are consistent with physisorption, while those around -40 kJ mol^{-1} or higher are associated with chemisorption as a result of the sharing or transfer of electrons from organic molecules to the metal surface to form a coordinate bond [55]. In the present work the value of ΔG°_{ads} is equal to -43.49 kJ mol^{-1}. The large value of ΔG°_{ads} and its negative sign is usually characteristic of strong interaction and a highly efficient adsorption [56]. The high value of ΔG°_{ads} shows that in the presence of 1.0 M HCl chemisorption of HPPTD may occur.

CONCLUSION

The present study shows that 3-hydroxy-7-isocyano-8-phenyl-2-(p-tolyl)pyrimido[2,1-b][1,3]thiazine-4,6-dione (HPPTD) functioned as an inhibitor of carbon steel corrosion in hydrochloric acid media. Polarization measurements suggest a mixed-inhibition mechanism, with predominant cathodic effectiveness. The protection efficiency of this inhibitor, calculated from impedance and polarization measurements, was found to increase with increase in concentration of the inhibitor showing a maximum efficiency of 94.7 % at 1.0 mM. The effect of temperature on the electrochemical system shows that the pyrimidothiazine derivative becomes less efficient at the highest temperature.

Adsorption models- Langmuir, Temkin and Frunkin isotherms were tested graphically for the data and the best fit was obtained with the Langmuir isotherm.

REFERENCES

[1] H.L. Wang, H.B. Fan, J.S. Zheng, *Mater. Chem. Phys*., **2002**, 77, 655.
[2] S.A. Abd El-Maksoud, A.S. Fouda, *Mater. Chem. Phys*., **2005**, 93, 84.
[3] M.A. Migahed, I.F. Nassar, *Electrochim. Acta*, **2008**, 53, 2877.
[4] M.A. Migahed, M. Abd-El-Raouf, A.M. Al-Sabagh, H.M. Abd-El-Bary, *Electrochim. Acta***, 2005**, 50, 4683.
[5] A. Zarrouk, H. Zarrok, R. Salghi, B. Hammouti, F. Bentiss, R. Touir, M. Bouachrine, *J. Mater. Environ. Sci.*, **2013**, 4, 177.
[6] M. Yadav, S. Kumar, U. Sharma, P.N. Yadav, *J. Mater. Environ*. Sci., *2013*, 4 (5), 691.
[7] A. K. Singh, M. A. Quraishi, *J. Mater. Environ. Sci.*, **2010**, 1, 101.
[8] U.J. Naik, V.A. Panchal, A.S. Patel, N.K. Shah, *J. Mater. Environ. Sci.*, **2012**, 3, 935.
[9] D. Ben Hmamou, R. Salghi, A. Zarrouk, H. Zarrok, S.S. Al-Deyab, O. Benali, B. Hammouti, *Int. J. Electrochem. Sci*., **2012**, 7, 8988.
[10] B. Hammouti, A. Zarrouk, S.S. Al-Deyab and I. Warad, *Orient. J. Chem*., 27 **(2011)** 23.
[11] A. Zarrouk, M. Messali, H. Zarrok, R. Salghi, A.A. Ali, B. Hammouti, S.S. Al-Deyab, F. Bentiss, *Int. J. Electrochem. Sci*., **2012**, 7, 6998.
[12] H. Zarrok, A. Zarrouk, R. Salghi, Y. Ramli, B. Hammouti, S. S. Al-Deyab, E. M. Essassi, H. Oudda, *Int. J. Electrochem. Sci*., **2012**, 7, 8958.
[13] A. Zarrouk, B. Hammouti, S.S. Al-Deyab, R. Salghi, H. Zarrok, C. Jama, F. Bentiss, *Int. J. Electrochem. Sci*., **2012,** 7, 5997.
[14] D. Ben Hmamou, M. R. Aouad, R. Salghi, A. Zarrouk, M. Assouag, O. Benali, M. Messali, H. Zarrok, B. Hammouti, *J. Chem. Pharm. Res*., **2012,** 4, 3489.
[15] A. Zarrouk, H. Zarrok, R. Salghi, B. Hammouti, S.S. Al-Deyab, R. Touzani, M. Bouachrine, I. Warad, T. B. Hadda, *Int. J. Electrochem. Sci*., **2012**, 7, 6353.
[16] H. Zarrok, R. Saddik, H. Oudda, B. Hammouti, A. El Midaoui, A. Zarrouk, N. Benchat, M. Ebn Touhami, *Der Pharm. Chem*., **2011**, 3, 272.
[17] A. Zarrouk, B. Hammouti, A. Dafali, H. Zarrok, *Der Pharm. Chem*., **2011**, 3, 266.
[18] A. Ghazoui, R. Saddik, N. Benchat, B. Hammouti, M. Guenbour, A. Zarrouk, M. Ramdani, *Der Pharm. Chem*., **2012**, 4, 352.
[19] A. Zarrouk, B. Hammouti, H. Zarrok, M. Bouachrine, K.F. Khaled, S.S. Al-Deyab, *Int. J. Electrochem. Sci*., **2012**, 6, 89.
[20] A. Zarrouk**,** B. Hammouti, H. Zarrok, I. Warad, M. Bouachrine, *Der Pharm. Chem*., **2011**, 3, 263.
[21] A. H. Al Hamzi, H. Zarrok, A. Zarrouk, R. Salghi, B. Hammouti, S. S. Al-Deyab, M. Bouachrine, A. Amine, F. Guenoun, *Int. J. Electrochem. Sci*., **2013**, 8, 2586.
[22] A. Ghazoui, N. Bencaht, S. S. Al-Deyab, A. Zarrouk, B. Hammouti, M. Ramdani, M. Guenbour, *Int. J. Electrochem. Sci*., **2013** 8, 2272.
[23] A. Zarrouk, H. Zarrok, R. Salghi, N. Bouroumane, B. Hammouti, S. S. Al-Deyab, R. Touzani, *Int. J. Electrochem. Sci*., **2012**, 7, 10215.
[24] H. Bendaha, A. Zarrouk, A. Aouniti, B. Hammouti, S. El Kadiri, R. Salghi, R. Touzani, *Phys. Chem. News*, **2012**, 64, 95.
[25] D. Ben Hmamou, R. Salghi, A. Zarrouk, B. Hammouti, S.S. Al-Deyab, Lh. Bazzi, H. Zarrok, A. Chakir, L. Bammou, *Int. J. Electrochem. Sci*., **2012**, 7, 2361.
[26] S.A. Abd El-Maksoud, A.S. Fouda, *Mater. Chem. Phys*., **2005**, 93, 84.
[27] K.F. Khaled, *Electrochim. Acta*, **2003**, 48, 2493.
[28] A. Popova, M. Christov, S. Raicheva, E. Sokolova, *Corros. Sci*., **2004**, 46, 1333.
[29] M. ELbakri, R. Touir, M. Ebn Touhami, A. Srhiri, , M. Benmessaoud, *Corros. Sci.*, **2008**, 50, 1538.
[30] M. Cenoui, N. Dkhireche, O. Kassou, M. Ebn Touhami, R. Touir, A. Dermaj, N. Hajjaji, *J. Mater. Environ. Sci.*, **2010**, 1, 84.
[31] J. Hmimou, A. Rochdi, R.Touir, M. Ebn Touhami, E.H. Rifi, A. El Hallaoui, A. Anouar, , D. Chebab, *J. Mater. Environ. Sci.*, **2012**, 3, 543.
[32] F. Bentiss, M. Lebrini, M. Lagrenee, *Corros. Sci*., **2005**, 47, 2915.
[33] S. Issaadi, T. Douadi, A. Zouaoui, S. Chafaa, M.A. Khan, G. Bouet, *Corros. Sci*., **2011**, 53, 1484.
[34] H. Serrar, S. Boukhris, A. Hassikou and A. Souizi, *J. Heterocyclic Chem*., **2013**, DOI 10.1002/jhet.2085
[35] H. Zarrok, A. Zarrouk, B. Hammouti, R. Salghi, C. Jama, F. Bentiss, *Corros. Sci*., **2012**, 64, 243.
[36] S. S. Abd El Rehim, H. H. Hassan, M. A. Amin, *Mater. Chem. Phys*., **2002**, 78, 337.
[37] Q. Zhang, Y. Hua, *Mater. Chem. Phys*., **2010**, 119, 57.
[38] K. F. Khaled, *Corros. Sci*., **2010**, 52, 2905.

[39] H. Amar, T. Braisaz, D. Villemin, B. Moreau, *Mater. Chem. Phys*., **2008**, 110, 1.
[40] D. Gopi, K. M. Govindaraju, L. Kavitha, *J. Appl. Electrochem*., **2010**, 40, 1349.
[41] R. Solmaz, E. Altunbas, G. Kardas, *Mater. Chem. Phys*., **2011**, 125, 796.
[42] A. Chetouani, A. Aouniti, B. Hammouti, N. Benchat, T. Benhadda, S. Kertit, *Corros. Sci*., **2003**, 45, 1675.
[43] D.A. Lopez, S.N. Simison, S.R. de Sanchez, *Electrochim. Acta*, **2003**, 48, 845.
[44] Z.H. Tao, S.T. Zhang, W.H. Li, B.R. Hou, *Corros. Sci*., **2009**, 51, 2588.
[45] E.S. Ferreira, C. Giacomelli, F.C. Giacomelli, A. Spinelli, *Mater. Chem. Phys*., **2004**, 83, 129.
[46] M. Lebrini, F. Robert, A. Lecante, C. Roos, *Corros. Sci*., **2011**, 53, 687.
[47] G. Moretti, G. Quartaronr, A. Tassan, A. Zingales, *Electrochim. Acta*, **1996**, 41, 1971.
[48] S. Martinez, I. Stern, *J. Appl. Electrochem*., **2001**, 31, 973.
[49] S.S. Abd El-Rehim, M.A.M. Ibrahim, K.F. Khaled, *Mater. Chem. Phys*., **2001**, 70, 268.
[50] N.M. Guan, L. Xueming, L. Fei, *Mater. Chem. Phys*., **2004**, 86, 59.
[51] S. Martinez, I. Stern, *Appl. Surf. Sci*., **2002**, 199, 83.
[52] N. Hackerman and E. McCafferty, Proceeding of the fifth International Congress on Mettalic Corrosion, Tokyo, **1972**, 542.
[53] R. Solmaz, G. Kardas, M. Culha, B. Yazici, M. Erbil, *Electrochim. Acta,* **2008**, 53, 5941.
[54] O. Olivares, N.V. Likhanova, B. Gomez, J. Navarrete, M.E. Llanos-Serrano, E. Arce, J.M. Hallen, *Appl. Surf. Sci*.**, 2006**, 252, 2894.
[55] S.A. Refay, F. Taha, A.M. Abd El-Malak, *Appl. Surf. Sci.*, **2004**, 236, 175.
[56] M. Abdallah, *Corros. Sci*., **2002**, 44, 717.